Received: 26 March 2020 | Revised: 11 June 2020 | Accepted: 2 July 2020

DOI: 10.4218/etrij.2020-0118

ORIGINAL ARTICLE

ETRI Journal WILEY

E-band low-noise amplifier MMIC with impedance-controllable filter using SiGe 130-nm BiCMOS technology

Woojin Chang[1] | **Jong-Min Lee**[1] | **Seong-Il Kim**[2] | **Sang-Heung Lee**[2] | **Dong Min Kang**[1]

[1]RF/Power Component Research Section, Electronics and Telecommunications Research Institute, Daejeon, Rep. of Korea

[2]Defense Materials and Components Convergence Research Department, Electronics and Telecommunications Research Institute, Daejeon, Rep. of Korea

Correspondence
Woojin Chang, RF/Power Component Research Section,Electronics and Telecommunications Research Institute, Daejeon, Rep. of Korea.
Email: wjchang@etri.re.kr

Funding information
Civil Military Technical Cooperation Program, Grant/Award Number: No. 18-CM-SS-12

Abstract

In this study, an E-band low-noise amplifier (LNA) monolithic microwave integrated circuit (MMIC) has been designed using silicon-germanium 130-nm bipolar complementary metal-oxide-semiconductor technology to suppress unwanted signal gain outside operating frequencies and improve the signal gain and noise figures at operating frequencies. The proposed impedance-controllable filter has series (R_s) and parallel (R_p) resistors instead of a conventional inductor-capacitor (L-C) filter without any resistor in an interstage matching circuit. Using the impedance-controllable filter instead of the conventional L-C filter, the unwanted high signal gains of the designed E-band LNA at frequencies of 54 GHz to 57 GHz are suppressed by 8 dB to 12 dB from 24 dB to 26 dB to 12 dB to 18 dB. The small-signal gain S_{21} at the operating frequencies of 70 GHz to 95 GHz are only decreased by 1.4 dB to 2.4 dB from 21.6 dB to 25.4 dB to 19.2 dB to 24.0 dB. The fabricated E-band LNA MMIC with the proposed filter has a measured S_{21} of 16 dB to 21 dB, input matching (S_{11}) of –14 dB to –5 dB, and output matching (S_{22}) of –19 dB to –4 dB at E-band operating frequencies of 70 GHz to 95 GHz.

KEYWORDS

E-band, impedance-controllable filter, low-noise amplifier, unwanted signal suppression

1 | INTRODUCTION

The licensed E-band frequency ranges of 71 GHz to 76 GHz, 81 GHz to 86 GHz, and 92 GHz to 95 GHz are of considerable value in high-data-rate networks, point-to-point wireless local area networks, remote sensing systems, imaging radar systems, atmospheric monitoring systems, avionic radar applications, and radio astronomy [1]. Millimeter-wave radar and wireless local area network systems need to be small and involve inexpensive components. In particular, at high operating frequencies such as E-band frequencies, monolithic microwave integrated circuit (MMIC) technologies present notable advantages such as a low cost and small size for mass production and realize high yield and reliability compared to hybrid integrated circuit technologies [2]. Some of these applications, including large-scale products and cost-effective components fabricated using silicon-based technologies, are required. Some recent integrated circuits for E-band frequencies have been based on complementary metal-oxide-semiconductor (CMOS) and silicon-germanium (SiGe) bipolar CMOS (BiCMOS) technologies [1,2]. Among the components in these systems, a low-noise amplifier (LNA) is a key component located at the front of a receiver that improves the overall noise figures of these systems and increases the initial signal power gain from the antenna. However,

some LNAs in these systems exhibit problems regarding the unwanted overly high signal gain at frequencies below operating frequencies. The performance of systems using LNAs that have such an unwanted gain can be degraded by the intermodulation distortion of the signals at operating frequencies and the high signals below operating frequencies. To solve these LNA problems, direct current (DC) biasing circuits in LNAs were designed to suppress the unwanted signal gain at low frequencies [3] and an inductor-capacitor (L-C) resonator was used to filter unwanted system interference [4]. In this study, a SiGe 130-nm BiCMOS E-band LNA MMIC was designed to suppress unwanted signal gain below operating frequencies and improve the signal gain characteristics at operating frequencies using an impedance-controllable filter in an interstage matching circuit.

2 | LNA DESIGN

2.1 | Device technology

The LNA was designed and fabricated using IHP's SiGe 130-nm BiCMOS technology (IHP SG13S). The high-speed SiGe heterojunction bipolar transistor (HBT) for LNA design has an emitter area of 4 × 120 nm × 480 nm, a current gain of 900 A/A, a cutoff frequency f_T of 240 GHz, a maximum oscillation frequency f_{max} of 340 GHz, and a collector-emitter breakdown voltage BV_{CEO} of 1.65 V.

2.2 | LNA design

A single-stage LNA with a common-emitter structure was designed using the SiGe HBT with an emitter area of 4 × 120 nm × 480 nm, as shown in Figure 1. The simulated bias conditions of the single-stage LNA were a collector-emitter voltage V_{CE} of 1.2 V, a base-emitter voltage V_{BE} of 0.9 V, and a collector-emitter current I_{CE} of 3 mA. For unconditionally stable operation, it was designed using the resistor-capacitor (R-C) pair composed of R_2 and C_3 in parallel, as displayed in Figure 1, and using the microstrip line L_5 as an inductor between the HBT emitter and ground [5–9]. L_5 also modifies the series inductive feedback so it is close the minimum noise point and the maximum available gain of the HBT to achieve more gain and lower noise figures in the LNA [10,11]. The matching and DC bias circuits of the LNA were designed with microstrip lines, metal-insulator-metal (MIM) capacitors, and a resistor. The MIM capacitors, C_1 and C_5, act as DC-blocking and radio-frequency (RF)-coupling and -matching elements. Figure 2 shows the simulated gain circles and noise figure circles of the designed single-stage LNA at 94 GHz. When the input matching circuit of the single-stage LNA was designed to the point of Γ_S, the LNA attained a 4-dB gain and 5-dB noise figure at 94 GHz, as indicated in Figure 2. The simulated small-signal gains S_{21} of the single-stage LNA were 4.1 dB to 4.6 dB at 70 GHz to 95 GHz, as shown in Figure 3. The simulated input and output matchings (S_{11} and S_{22}) of the single-stage LNA were –19 dB to –5 dB and –28 dB to –14 dB, respectively, at 70 GHz to 95 GHz. The simulated noise figures of the single-stage LNA were 5.1 dB to 5.9 dB at 70 GHz to 95 GHz.

A four-stage LNA with a common-emitter structure was designed and optimized using the designed single-stage LNA, as shown in Figure 4. The simulated bias conditions of the four-stage LNA were V_{CE} = 1.2 V, V_{BE} = 0.9 V, and I_{CE} = 12 mA. The simulated S_{21} and noise figures of the four-stage LNA were 21.6 dB to 25.4 dB and 5.3 dB to 6.2 dB, respectively, at 70 GHz to 95 GHz, as indicated in Figure 5. The simulated S_{11} and S_{22} of the four-stage LNA were –15 dB to –4 dB and –24 dB to –5 dB, respectively, at 70 GHz to

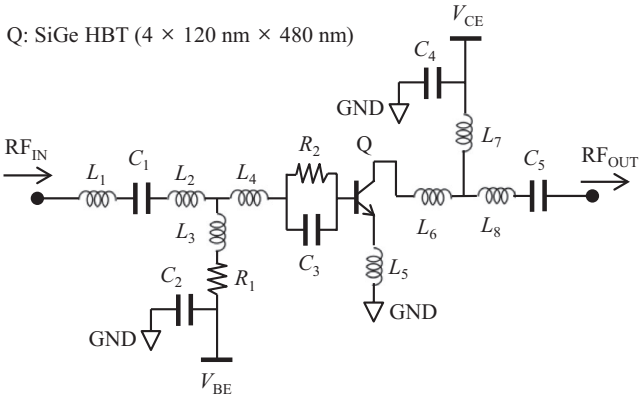

FIGURE 1 Schematic of the designed single-stage LNA

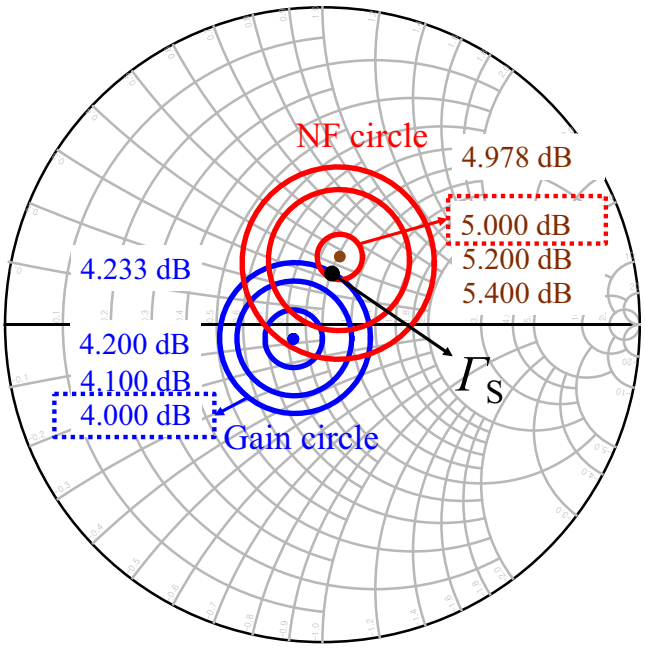

FIGURE 2 Simulated gain circle and noise figure circle of the single-stage LNA at 94 GHz

95 GHz, as displayed in Figure 5. In Figure 5, some unwanted high signal gains at frequencies of 54 GHz to 57 GHz below the operating frequencies of 70 GHz to 95 GHz were simulated at 24.5 dB to 26.1 dB. These unwanted out-of-band signal gains degrade the performance of the system. Therefore, high signal gains outside the operating frequencies should be suppressed by a low-pass filter or a resonator. In this study, the four-stage LNA has been designed to suppress the high small-signal gain at 54 GHz to 57 GHz and to flatten the small-signal gain at operating frequencies using the impedance-controllable filter described in Section 2.3.

2.3 | Filter design

A conventional L-C filter is composed of an inductor (with inductance L) and capacitor (with capacitance C), as displayed in Figure 6A.

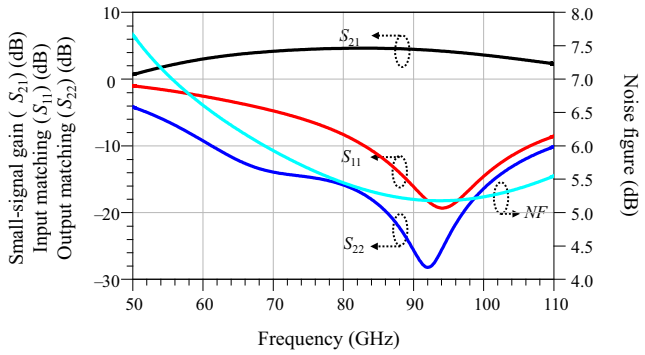

FIGURE 3 Simulated small-signal and noise figure characteristics of the single-stage LNA

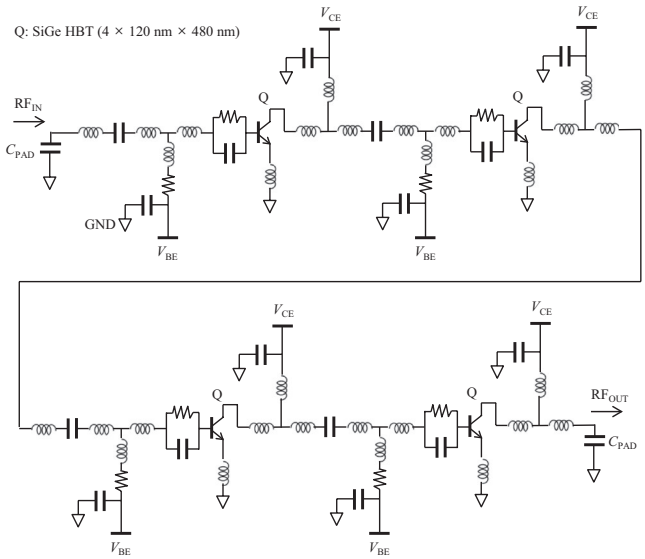

FIGURE 4 Schematic of the designed four-stage LNA

The conventional L-C filter theoretically has an impedance of zero at the resonance frequency and very low impedances at frequencies adjacent to the resonance frequency, expressed as follows:

$$z_1 = j\omega\left(L - \frac{1}{\omega^2 C}\right). \tag{1}$$

Therefore, when the conventional L-C filter is applied to the matching circuit in the amplifier, the RF signals at the resonance frequency flow through the filter to ground; eventually, the RF signal gain of the amplifier at the resonance frequency decreases too much. In some cases, even at operating frequencies adjacent to the resonance frequency, the RF signal gains of the amplifier with the L-C filter are also decreased. The RF signals flowing through the L-C filter to ground can be reduced by increasing the impedances of the filter at the resonance frequency and at operating

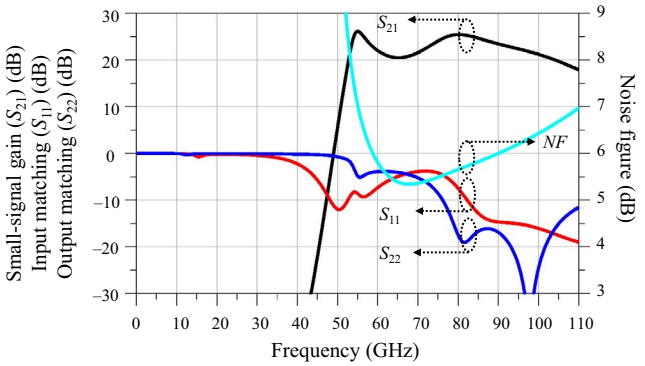

FIGURE 5 Simulated small-signal and noise figure characteristics of the four-stage LNA

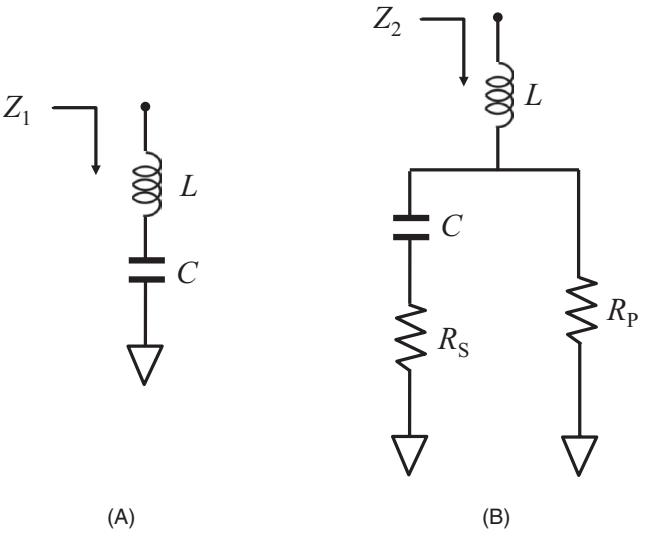

FIGURE 6 (A) Conventional L-C filter and (B) proposed filter with resistors having resistances of R_S and R_P

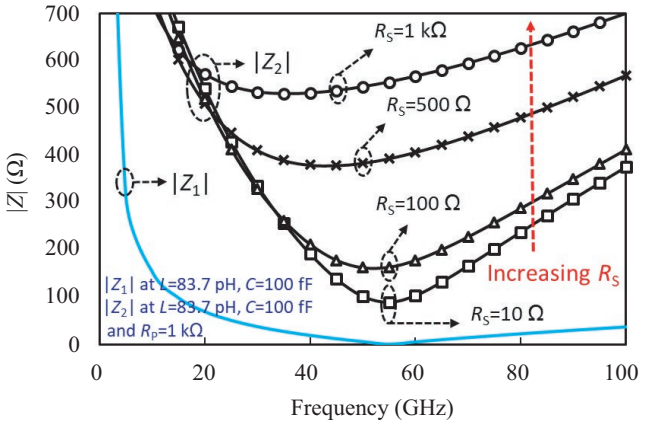

FIGURE 7 $|Z_1|$ of the conventional L-C filter and $|Z_2|$ of the proposed impedance-controllable filter with R_S and R_P

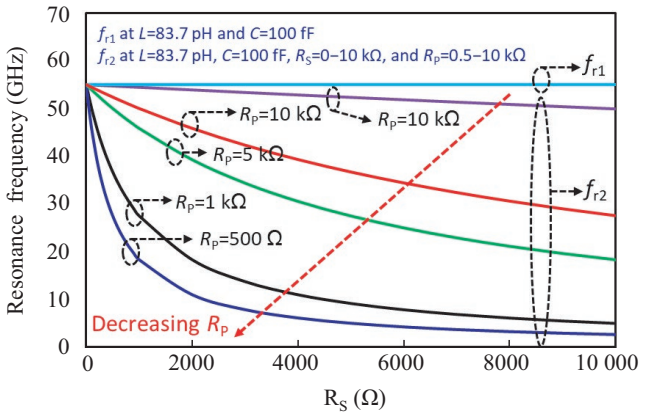

FIGURE 8 f_{r1} of the conventional L-C filter and f_{r2} of the proposed filter with R_S and R_P for $R_S = 0$–10 kΩ

frequencies adjacent to the resonance frequency, which can improve the RF signal gain characteristics of an amplifier with unwanted overly high signal gains outside the operating frequencies. To increase $|Z_1|$ of the conventional L-C filter to more than zero at the resonance frequency, an impedance-controllable filter with two additional resistors (with resistances R_S and R_P) is proposed, as shown in Figure 6B. The impedance Z_2 and resonance frequency f_{r2} of the impedance-controllable filter were compared with the impedance Z_1 and resonance frequency f_{r1} of the conventional L-C filter using (2)–(4). $|Z_1|$ of the conventional L-C filter with an inductance of 83.7 pH and a capacitance of 100 fF is zero at 55 GHz, and $|Z_2|$ of the proposed filter with an inductance of 83.7 pH, a capacitance of 100 fF, R_S = 10–1000 Ω, and R_P = 1 kΩ is 90 to 560 Ω at 55 GHz per (1) and (2). Figure 7 presents $|Z_1|$ of the conventional L-C filter and $|Z_2|$ of the proposed filter with R_S and R_P for frequencies of 0 to 100 GHz.

$$z_2 = \frac{R_P + \omega^2 C^2 R_S R_P (R_S + R_P)}{1 + \omega^2 C^2 (R_S + R_P)^2} + j\omega \left(L - \frac{C R_P^2}{\omega^2 C^2 (R_S + R_P)^2} \right), \tag{2}$$

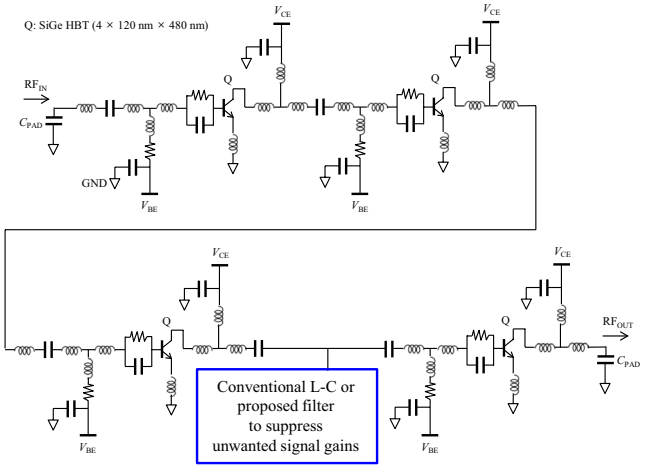

FIGURE 9 Schematic of the four-stage LNA with the conventional L-C or proposed filter

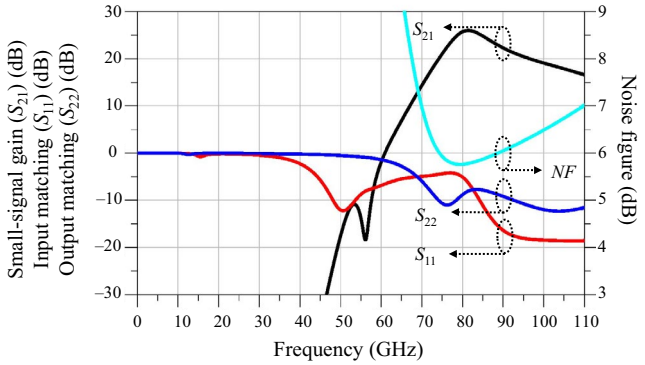

FIGURE 10 Simulated small-signal and noise figure characteristics of the four-stage LNA with the conventional L-C filter

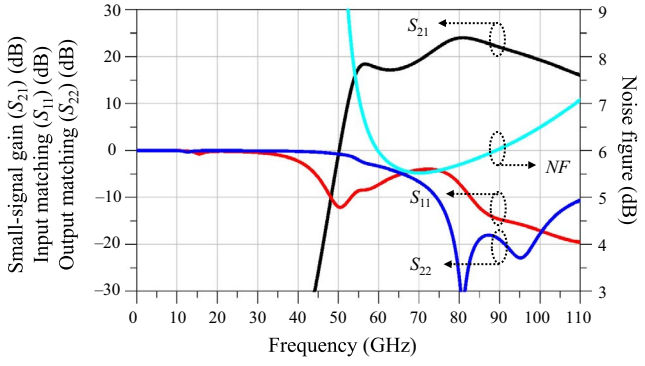

FIGURE 11 Simulated small-signal and noise figure characteristics of the four-stage LNA with the proposed filter using the R_S and R_P

$$f_{r1} = \frac{1}{2\pi\sqrt{LC}}, \tag{3}$$

$$f_{r2} = \frac{1}{2\pi(R_S + R_P)} \sqrt{\frac{CR_P^2 - L}{LC^2}}. \tag{4}$$

TABLE 1 Simulated signal gains of three designed LNAs

	Signal gain (S_{21}) at operating frequency (70 GHz to 95 GHz)	Signal gain (S_{21}) at unwanted frequency (54 GHz to 57 GHz)
LNA without any filter (dB)	21.6 to 25.6	24.5 to 26.1
LNA with conventional L-C filter (dB)	14.4 to 26.0	−18.4 to 11.2
LNA with proposed impedance-controllable filter (dB)	19.2 to 24.0	15.5 to 18.4

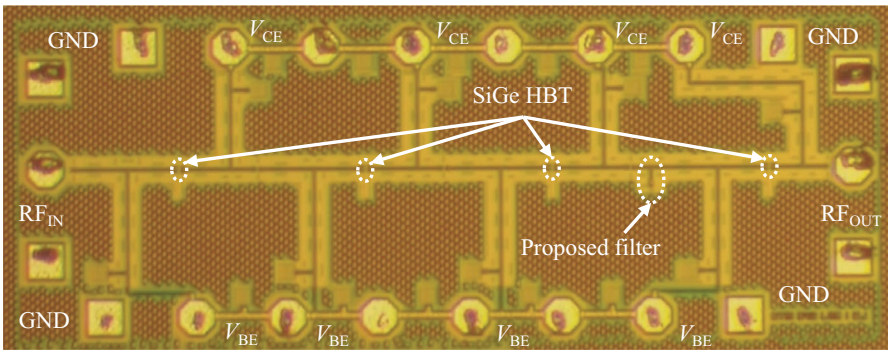

FIGURE 12 Photograph of the fabricated E-band four-stage LNA MMIC with the proposed filter

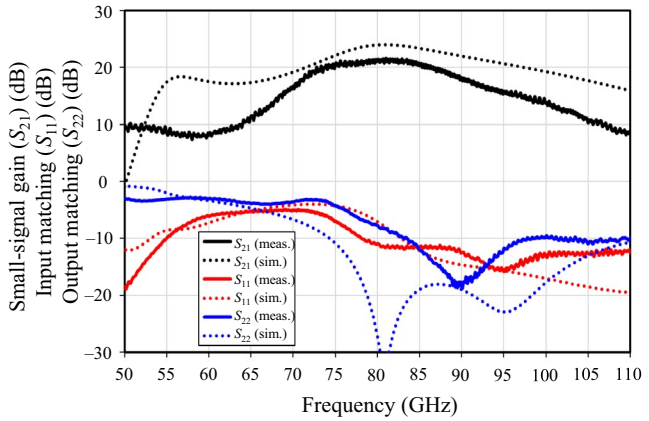

FIGURE 13 Measured small-signal gain and input/output matchings compared with the simulated results of the E-band four-stage LNA with the proposed filter

f_{r1} of the conventional L-C filter with an inductance of 83.7 pH and a capacitance of 100 fF is 55 GHz, and f_{r2} of the proposed filter with an inductance of 83.7 pH, a capacitance of 100 fF, R_S = 0–10 kΩ, and R_P = 0.5–10 kΩ is 2 to 55 GHz per (3) and (4). Figure 8 presents f_{r1} of the conventional L-C filter and f_{r2} of the proposed filter with R_S and R_P for R_S = 0–10 kΩ. Even if the inductance and capacitance in the impedance-controllable filter have been not changed, the resonance frequencies and impedances are controlled because R_S and R_P change as indicated in Figures 7 and 8. Smaller values of R_P in the proposed filter result in a greater resonance frequency range, as shown in Figure 8. The resonance frequency and impedance of the impedance-controllable filter can be changed by R_S and R_P, while the resonance frequency and impedance of the conventional L-C filter are fixed at the value given in (3) and zero at the resonance frequency, respectively.

2.4 | LNA design with impedance-controllable filter

Figure 9 shows the conventional L-C or proposed filter applied to the designed four-stage LNA to improve the RF signal gain characteristics of the LNA with unwanted overly high signal gains at 54 GHz to 57 GHz.

The conventional L-C filter was designed with L = 83.7 pH and C = 100 fF. The simulated S_{21} and noise figures of the four-stage LNA with the conventional L-C filter were 14.4 dB to 26.0 dB and 5.8 dB to 7.0 dB, respectively, at 70 GHz to 95 GHz, as shown in Figure 10. The simulated S_{11} and S_{22} were –18 dB to –4 dB and –11 dB to –6 dB, respectively, at 70 GHz to 95 GHz, as shown in Figure 10. In Figure 10, because $|Z_1|$ of the conventional L-C filter with 83.7 pH and 100 fF is zero at a resonance frequency of 55 GHz, some unwanted signal gains at 54 GHz to 57 GHz were suppressed by 37.3 dB to 42.9 dB compared with Figure 5. However, the values of S_{21} at operating frequencies also decreased by –0.6 dB to 7.2 dB from 21.6 dB to 25.4 dB to 14.4 dB to 26.0 dB compared with those in Figure 5. The simulated noise figures of the four-stage LNA were 5.8 dB to 7.0 dB at 70 GHz to 95 GHz, as displayed in Figure 10. The noise figures at operating frequencies of 70 GHz to 95 GHz also increased by 0.5 dB to 0.8 dB compared with the noise figures of the designed LNA without any filter.

The proposed filter was applied to the designed four-stage LNA to improve the RF signal gain characteristics of the LNA with unwanted overly high signal gains at 54 GHz to 57 GHz. The impedance-controllable filter was designed so that $L = 83.7$ pH, $C = 100$ fF, $R_S = 100$ Ω, and $R_P = 1$ kΩ, and $|Z_2|$ is 92 Ω at a resonance frequency of 50 GHz for these parameters. Using the nonzero impedance characteristic of the impedance-controllable filter in the matching circuit between the third and fourth stages in the four-stage LNA, the RF signal gain characteristics with the overly high signal gain at 54 GHz to 57 GHz and the poor gain flatness at 70 GHz to 95 GHz were improved, as shown in Figure 11. The simulated S_{21} and noise figures of the four-stage LNA with the proposed filter were 19.2 dB to 24.0 dB and 5.5 dB to 6.2 dB, respectively, at 70 GHz to 95 GHz, as displayed in Figure 11. The simulated S_{11} and S_{22} were –16 dB to –4 dB and –33 dB to –7 dB, respectively, at 70 GHz to 95 GHz, as indicated in Figure 11. The noise figures at operating frequencies of 70 GHz to 95 GHz were also increased by 0.0 dB to 0.2 dB compared with the noise figures of the designed LNA without any filter. In Figure 11, some unwanted signal gains at frequencies of 54 GHz to 57 GHz were suppressed by 7.7 dB to 9.0 dB from 24.5 dB to 26.1 dB to 15.5 dB to 18.4 dB compared with those in Figure 5. S_{21} at the operating frequencies were only decreased by 1.4 dB to 2.4 dB from 21.6 dB to 25.4 dB to 19.2 dB to 24.0 dB compared with that in Figure 5. The proposed impedance-controllable filter with nonzero impedance in the four-stage LNA has better signal gain characteristics and noise figures than the conventional L-C filter in the four-stage LNA when suppressing the unwanted signal gain and widening the operating frequencies. Table 1 summarizes the simulated signal gains of the three designed LNAs.

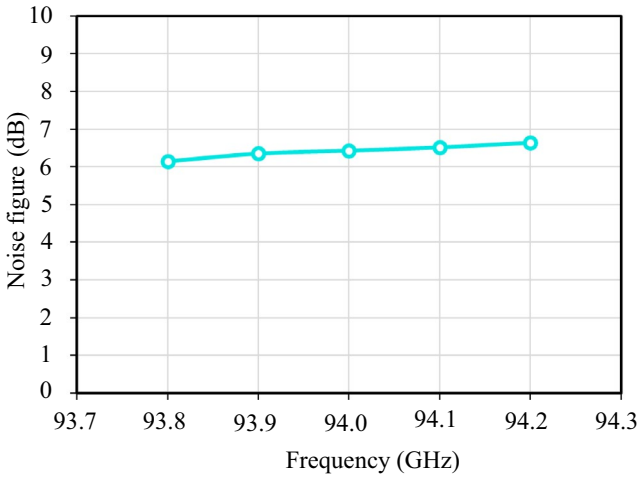

FIGURE 14 Measured noise figure of the fabricated E-band four-stage LNA with the proposed filter

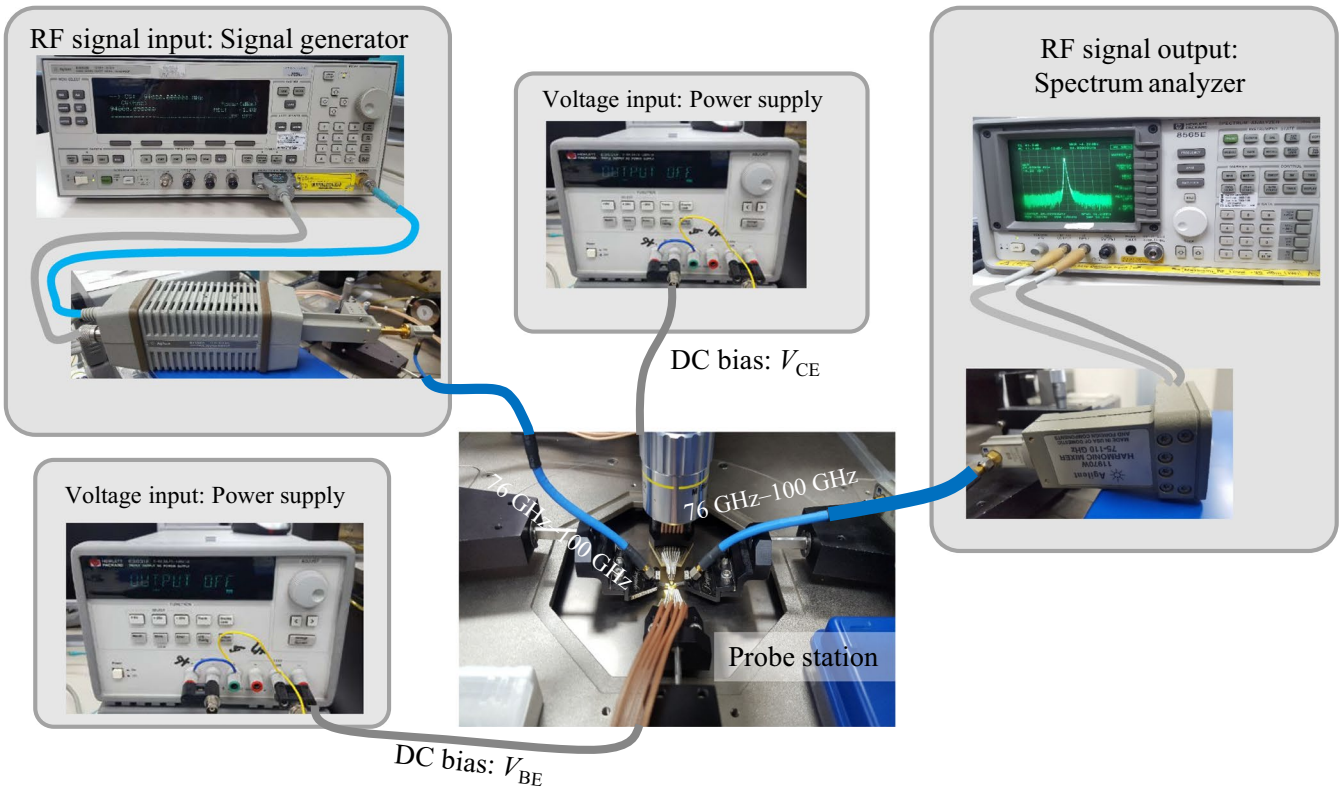

FIGURE 15 Photograph of the large-signal on-wafer measurement setup

3 | MEASUREMENTS

3.1 | Fabrication

Figure 12 shows a photograph of the fabricated E-band four-stage LNA MMIC with the proposed filter using two additional resistors using IHP's SiGe 130-nm BiCMOS technology (IHP SG13S). The chip area of the LNA is 1.38 mm × 0.54 mm (0.74 mm^2), including two RF ground-signal-ground (GSG) pads and the DC pads.

3.2 | Small-signal measurements

Anritsu's MS4647A vector network analyzer and Anritsu's 3743A millimeter-wave module were used to obtain the small-signal characteristics at frequencies of 70 GHz to 95 GHz. Under the DC bias conditions of the fabricated LNA MMIC, V_{CE} = 1.2 V, V_{BE} = 0.9 V, I_{CE} = 13 mA, and P_{DC} = 15.6 mW. The fabricated E-band LNA MMIC has a measured S_{21} of 16 dB to 21 dB, S_{11} of –16 dB to –5 dB, and S_{22} of –19 dB to –4 dB for the E-band operating frequencies of 70 GHz to 95 GHz, as displayed in Figure 13. There was a difference of 1 dB to 5 dB between the simulated and measured S_{21} at 70 GHz to 95 GHz. This might be due to the degradation in the output matching characteristics compared with the simulated S_{22} and underestimation of the via resistances in the simulation. The fabricated E-band LNA with the proposed impedance-controllable filter has been able to effectively suppress the unwanted signal gain at 54 GHz to 57 GHz, although this unwanted signal gain was more suppressed than in the simulation. Noisecom's NC5110A noise source and SAGE's W-band varactor-tuned Gunn oscillator were used to obtain the noise figure characteristics of the fabricated LNA MMIC at frequencies of 93.8 GHz to 94.2 GHz, as displayed in Figure 14. The frequency range of the noise figure measurements was limited to 93.8 GHz to 94.2 GHz, which has been already verified by the measurement system. The LNA MMIC has a measured noise figure of 6.2 dB to 6.6 dB at 93.8 GHz to 94.2 GHz.

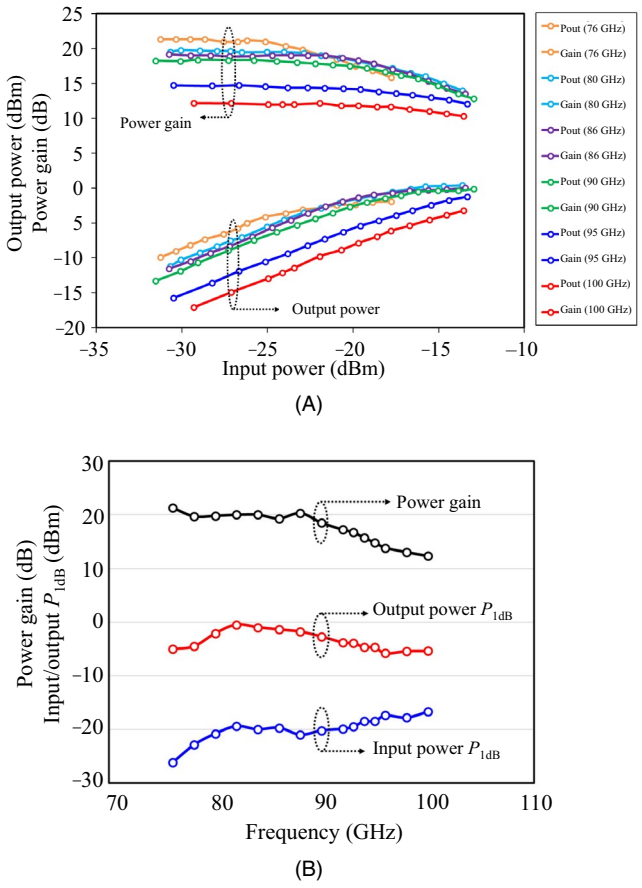

FIGURE 16 Measured power gain and power characteristics of the fabricated E-band four-stage LNA with the proposed filter: (A) power gain and output power according to the input power and (B) power gain and input/output P_{1dB} for 76 GHz to 100 GHz

3.3 | Large-signal measurements

Figure 15 shows the large-signal on-wafer measurement setup for the fabricated E-band four-stage LNA MMIC. Keysight's 83650B signal generator and 83558A millimeter-wave source module were used for the large-signal source at frequencies of 76 GHz to 100 GHz. Keysight's 8365E spectrum analyzer and 11970W harmonic mixer were used for large-signal measurement at frequencies of 76 GHz to 100 GHz. The large-signal continuous-wave (CW) behavior of the fabricated LNA was measured at 76 GHz to 100 GHz, as shown in Figure 16. The fabricated E-band LNA MMIC has a measured power gain of 12 dB to 21 dB, an input 1-dB compression power P_{1dB} of –26 dBm to –17 dBm, and an output P_{1dB} of –5 dBm to –1 dBm at 76 GHz to 100 GHz.

4 | CONCLUSIONS

In this study, a SiGe 130-nm BiCMOS E-band LNA MMIC has been designed to suppress unwanted signal gain at 54 GHz to 57 GHz outside the operating frequencies of 70 GHz to 95 GHz and improve the signal gains and noise figures at these operating frequencies. The proposed impedance-controllable filter was used instead of the conventional L-C filter in the interstage matching circuit of the LNA. The impedance-controllable filter consists of one series resistor and one parallel resistor between the inductor and the capacitor in the conventional L-C filter. The impedance of the impedance-controllable filter can be changed by these two resistors, while the impedance of the conventional L-C filter is zero at the resonance frequency. The fabricated E-band LNA MMIC with the impedance-controllable filter has a measured S_{21} of 16 dB to

21 dB, S_{11} of –16 dB to –5 dB, and S_{22} of –19 dB to –4 dB for the E-band operating frequencies of 70 GHz to 95 GHz. The fabricated LNA MMIC has a measured power gain of 12 dB to 21 dB, an input P_{1dB} of –26 dBm to –17 dBm, and an output P_{1dB} of –5 dBm to –1 dBm at 76 GHz to 100 GHz.

ORCID

Woojin Chang https://orcid.org/0000-0003-0911-3709
Jong-Min Lee https://orcid.org/0000-0002-0946-0615

REFERENCES

1. W. Winkler et al., *94 GHz amplifier in SiGe technology*, in Proc. Eur. Microw. Conf. (Amsterdam, Netherlands), Oct. 2008, pp. 167–170.
2. W. T. Khan et al., *A 94 GHz flip-chip packaged SiGe BiCMOS LNA on an LCP Substrate*, in Proc. IEEE MTT-S Int. Microw. Symp. Digest (Seattle, WA, USA), June 2013, https://doi.org/10.1109/MWSYM.2013.6697744
3. M. Sarkar, P. Banerjee, and A. Majumder, *Design of broadband MMIC low noise amplifier at W band using GaAs pHEMTs*, in Proc. Int. Conf. Innovations Electron. Signal Process. Commun. (Shilong, India), Apr. 2017, pp. 194–198.
4. K. Kwon, S. Kim, and K. Y. Son, *A hybrid transformer-based CMOS duplexer with a single-ended notch-filtered LNA for highly integrated tunable RF front-ends*, IEEE Microw. Wirel. Compon. Lett. **28** (2018), 1032–1034.
5. W. Chang et al., *Design and implementation of 40-GHz-band LNA MMICs with super low-gain flatness*, J. Korean Phys. Soc. **40** (2002), 552–556.
6. D. Elad, R. Shaulsky, and B. Mezhebovsky, *A novel method for even odd parametric oscillation stability analysis of a microwave power amplifier*, in Proc. IEEE MTT-S Microw. Symp. Digest (San Francisco, CA, USA), June 2006, pp. 1850–1854.
7. A. Anakabe et al., *Analysis and elimination of parametric oscillations in monolithic power amplifier*, in IEEE MTT-S Microw. Symp. Digest (Seattle, WA, USA), June 2002, 2181–2184.
8. D. Teeter, A. Platzker, and R. Bourque *A compact network for eliminating parametric oscillations in high power MMIC amplifiers*, in Proc. IEEE MTT-S Microw. Symp. Digest (Anaheim, CA, USA), June 1999, pp. 967–970.
9. D. Shin, I. Yom, and D. Kim, *6-GHz-to-18-GHz AlGaN/GaN cascaded nonuniform distributed power amplifier MMIC using load modulation of increased series gate capacitance*, ETRI J. **39** (2017), 737–745.
10. M. Gholami and M. C. E. Yagoub, *New stabilization technique to prevent parametric oscillations in a 35 W C-band AlGaN/GaN MMIC high power amplifier*, Progr. Electromagn. Res. C **86** (2018), 97–110.
11. W. Chang et al., *X-band MMIC low-noise amplifier MMIC on SiC substrate using 0.25-μm AlGaN/GaN HEMT technology*, Microw. Opt. Technol. Lett. **56** (2014), 96–99.

AUTHOR BIOGRAPHIES

Woojin Chang received his BS and MS degrees in information engineering from Korea University, Sejong, Rep. of Korea, in 1996 and 1998, respectively, and his PhD degree in electronic engineering from Chungnam National University, Daejeon, Rep. of Korea, in 2008. From 1998 to 1999, he worked as a research engineer at LG Precision, Yongin, Rep. of Korea, where he was engaged in R&D on power amplifier modules for wireless communications. In 1999, he joined Electronics and Telecommunications Research Institute, Daejeon, Rep. of Korea, where he is currently a principal research member. Recently, his main research interests are MMICs and compound semiconductor devices based on GaN, GaAs, InP, SiGe, and Ga_2O_3.

Jong-Min Lee received his BS degree in material science and engineering from Korea University, Seoul, Rep. of Korea, in 1995, and his MS and PhD degrees in material science from Korea University, Seoul, Rep. Korea, in 1997 and 2001, respectively. Since 2001, he has been with the Electronics and Telecommunications Research Institute, Daejeon, Rep. of Korea, where he is now a principal researcher. Recently, he has been engaged in the development of InP mHEMT and GaN HEMT devices and MMICs for wireless telecommunications and radar systems. His main research interests are compound semiconductor devices and MMICs for their system applications.

Seong-Il Kim received his BS degree in electrical engineering from Hanyang University Seoul, Rep. of Korea, in 1998; his MS degree in electrical engineering from Korea Advanced Institute of Science and Technology, Daejeon, Rep. of Korea, in 2000; and his PhD degree in electrical engineering from Chungnam University, Daejeon, Rep. of Korea, in 2019. Since 2000, he has been with Electronics and Telecommunications Research Institute, Daejeon, Rep. of Korea, as a member of the research staff, where he has been engaged in research on optoelectronic digital IC designs and RF power amplifier designs. He is currently a director of the Defense RF Packaging Research Section. His main research interests are W-band SiGe RF MMIC designs and GaN MMIC designs for transceiver modules.

Sang-Heung Lee received BS, MS, and PhD degrees from the department of electronics engineering at Chungnam National University, Daejeon, Korea, in 1988, 1992, and 1998, respectively. From April 1998 to June 1999, he held a position as a post-doctoral researcher at Electronics and Telecommunications Research Institute (ETRI) and from March 2009 to February 2011, a position as an adjunct professor at Chungnam National University. He has been serving as a principal researcher at ETRI since July 1999, acting as the leader of the SiGe Devices and Circuits Team from 2005 to 2008. His research interests include design in the field of radio-frequency integrated circuits and high-speed analog/digital communication circuits, semiconductor device modeling, and SPICE parameter extraction and optimization. He has authored and coauthored 155 papers in international and domestic journals and conference proceedings. Moreover, he has had 70 patents on semiconductor devices and circuits. He is a member of IEIE, KICS, and KEES.

Dong Min Kang received his MS degree in electronic engineering from Kwangwoon University, Seoul, Rep. of Korea, in 1998, and his PhD degree in radio communication engineering from Chungbuk National University, Cheongju, Rep. of Korea in 2009. From 1998 to 2000, he was with MCC, Seoul, Rep. of Korea, where he worked on RF modules for wireless communication systems. In 2000, he joined Electronics and Telecommunications Research Institute, Daejeon, Rep. of Korea, where he participated in the study of micro/millimeter-wave MMIC design for wireless communication systems and radar systems, and is currently a director of the RF/Power Components Research Section. His research interests include MMIC design, RF front-end module design, and packaging.